

Fault Diagnosis in Hydrodynamic Components of Rotating Machinery Observing Changes in the Pressure Distribution

Marcus Vinicius Gomes Diniz Abrantes

COPPE/UFRJ – Cepel, Centro de Pesquisas de Energia Elétrica, P.O. Box 68007, 21944-970 Rio de Janeiro - RJ - Brasil
marvin@cepel.br

José Bismark de Medeiros

COPPE/UFRJ – Cepel, Centro de Pesquisas de Energia Elétrica, P.O. Box 68007, 21944-970 Rio de Janeiro - RJ - Brasil
bismark@cepel.br

Renato de Oliveira Rocha

CEPEL, Centro de Pesquisas de Energia Elétrica, P.O. Box 68007, 21944-970 Rio de Janeiro - RJ - Brasil
renato@cepel.br

Moysés Zindeluk

PEM-COPPE/UFRJ, Programa de Engenharia Mecânica, P.O. Box 68503, 21945-970 Rio de Janeiro - RJ - Brasil
moyses@ufrj.br

Abstract: *The Reynolds' hydrodynamic theory used for journal bearings can be extended to other components that work in a similar way in rotating machinery. Some of those components have a deformed circular shape, due to installation distortions, or due to external forces at the operation, predicted or not during the design stage. The changes in the geometry of these components can influence the dynamic behavior of a rotating machine, thus a model that allows simulations of that type of fault is proposed. With a small modification during the development of the equations of plain journal bearings, it is possible to obtain a mathematical model that determines the pressure distribution, including the imperfections in the bore of the component. Observing the modifications that appear in the pressure field, and comparing to the perfectly circular case, it is possible to evaluate the deformed configuration of the ring, relating the pressure gradients to the convergence and divergence regions in the lubricant flow. The pressure data acquisition in the time domain, measured in different positions along the circumference of the ring, can be used to evaluate the excitation due to the dynamic forces caused by the pressure field. An analysis of these signals in the frequency domain may reveal other characteristics of the excitation.*

Keywords: *Pressure Field, Hydrodynamic Theory, Rotating Machinery.*

1. Introduction

The monitoring and diagnosis of rotating machinery are of extreme importance to ensure the safe and reliable operation of the equipment. The rotordynamic modeling play a significant role in the field–diagnostics approach. Hence, a detailed study of rotordynamics demands accurate knowledge of mechanical elements that support the rotor, such as bearing, seals and dampers. The knowledge about hydrodynamic components is then required to the development of adequate models for fluid forces acting on rotor, allowing an accurate study of these machines behavior.

In this work, a model is proposed to evaluate the geometric condition of a hydrodynamic component by measuring the pressure of the fluid. First a mathematical model based on the hydrodynamic theory used in journal bearings is developed. This model includes geometry deviations of the circular shape of the component. Some computer simulations are done to evaluate how these geometric changes affect the pressure generated in the fluid film. At the end some considerations regarding turbulent flow are presented.

Figure 1 schematically depicts a region of a power generator turbine where a deformed ring is located. Between the stationary and the rotating ring there is a fluid flow combining hydrodynamics with a forced axial flow. The work presented here will not account for this axial flow.

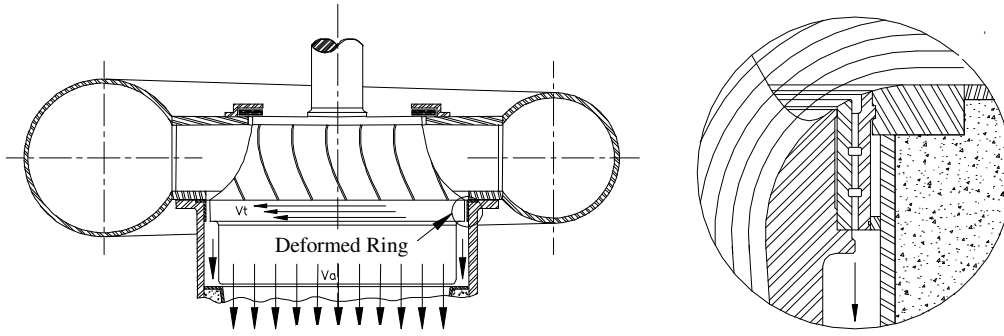


Figure 1. Detail of a power generator turbine

2. Mathematical Model.

In hydrodynamic fluid film bearings there is relative motion between two mechanical surfaces with a particular wedge shape. The fluid dragged due to the journal rotation is led to a convergent gap and hydrodynamic pressures able to support an externally applied load are generated. The development below describes the classical way to calculate the pressure generated in journal bearings.

2.1. Journal Bearing Model: Reynolds' Equation

The pressure p in the lubricant film of a journal bearings, as the illustrated in Fig. 2, is governed by the Reynolds equation, which is a simplified version of the Navier-Stokes equation and represents the conservation of mass across the film thickness. For such derivation some hypotheses must be made.

- The lubricant is an isoviscous, incompressible, Newtonian fluid.
- The curvatures of the surfaces can be neglected if compared to the film thickness (H).
- The film thickness is very small in comparison to the bearing circumference and length so that the pressure may be considered uniform in the y direction.
- The fluid adhere to the surfaces (non-slip condition).
- The flow is laminar and the inertia effects can be neglected

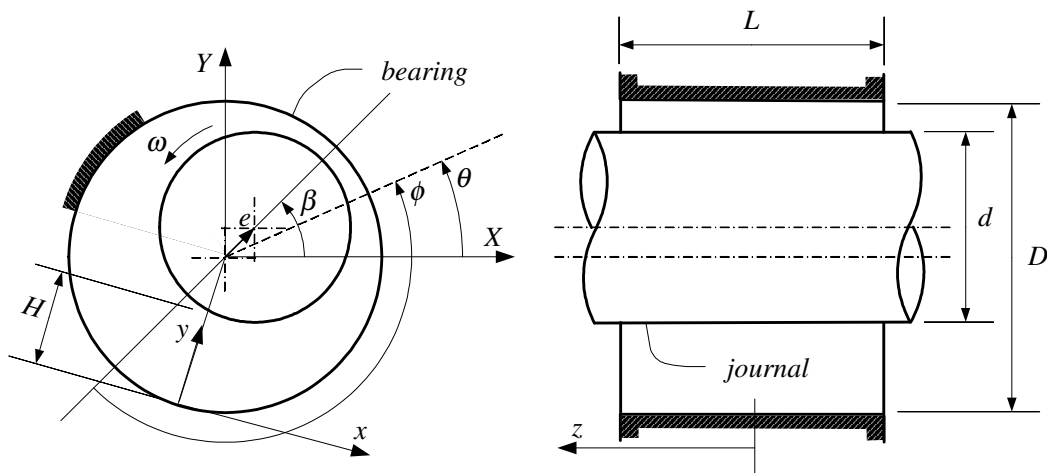


Figure 2. Geometry of a plain journal bearing

Equation (1) is the Reynolds equation for classical lubrication theory, written in circumferential coordinates where ω is the speed of rotation of the shaft, μ is the lubricant viscosity, r is the shaft radius, t it is the time and θ is the angular coordinate relative to the referential XY fixed on the bearing.

$$\frac{1}{r^2} \frac{\partial}{\partial \theta} \left(\frac{H^3}{12\mu} \frac{\partial p}{\partial \theta} \right) + \frac{\partial}{\partial z} \left(\frac{H^3}{12\mu} \frac{\partial p}{\partial z} \right) = \frac{\omega}{2} \frac{\partial H}{\partial \theta} + \frac{\partial H}{\partial t} \quad (1)$$

There is no analytical solution for Eq. (1), even if the bearing is perfectly circular. Numerical methods, as presented by Allaire et al (1977) and Childs (1993), have been employed for the direct solution of the Reynolds equation for various types of bearings. Some approximate solution have been used for quick estimations and one of them is presented in the following subsection.

2.2. The Ocvirk Solution (Short Bearing)

Some good approximate analytical solutions can be obtained if one of the terms on the left side is neglected. To decide which of the terms is dominant, the ratio between the shaft diameter (d) and the bearing length (L) must be evaluated. To evaluate this ratio influence in such approximations, the Reynolds equation is re-stated in terms of the following dimensionless variables:

$$z^* = \frac{z}{L}, \quad p^* = \left(\frac{c_r}{L}\right)^2 \frac{p}{12\mu\omega}, \quad t^* = \omega t, \quad h = \frac{H}{c_r} \quad (2)$$

where c_r is the radial clearance.

Substitution of Eq. (2) in Eq. (1) yields the following restatement of the Reynolds equation, where the ratio L/d appears in evidence in the first term.

$$4\left(\frac{L}{d}\right)^2 \frac{\partial}{\partial\theta} \left(h^3 \frac{\partial p^*}{\partial\theta} \right) + \frac{\partial}{\partial z^*} \left(h^3 \frac{\partial p^*}{\partial z^*} \right) = \frac{1}{2} \frac{\partial h}{\partial\theta} + \frac{\partial h}{\partial t^*} \quad (3)$$

Equation (3) demonstrates that the first term on the left become dominant for very long bearings. That means that the pressure gradient in the axial direction is very small if compared to the circumferential pressure gradient. On the other hand, for small L/d ratios, the first term becomes negligible. In this case the oil flow in the axial direction is much greater than in the circumferential direction.

Therefore, two different analytical solution for the Reynolds equation are possible. One for long bearings, known as Sommerfeld solution, and one for short bearings, known as Ocvirk solution. As most of the hydrodynamic components, specially bearings (Vance, 1988), fit the second case, this will be the chosen for the further development of the model. As mentioned by San Andres (2000), surprisingly good results are obtained with that approach as long as the ratio remains smaller than 0,5. Besides, the journal eccentricity should not be greater than 70% of the of the radial clearance value. The pressure field is obtained by integration of Eq. (4).

$$\frac{\partial}{\partial z} \left(\frac{H^3}{12\mu} \frac{\partial p}{\partial z} \right) = \frac{\omega}{2} \frac{\partial H}{\partial\theta} + \frac{\partial H}{\partial t} \quad (4)$$

Usually it is assumed that the pressure on the sides is the ambient pressure, and its maximum value occurs in the middle plane. The use of this information as boundary conditions for the integration leads to the following expression for the pressure field.

$$p = 3 \frac{\mu}{H^3} \left(2 \frac{\partial H}{\partial t} + \omega \frac{\partial H}{\partial\theta} \right) \left(z^2 - \frac{L^2}{4} \right) \quad (5)$$

The pressure field given by Eq. (5) is function of the film thickness (H) and its gradients. An expression for H is then necessary to calculate the pressure field.. From this point on, considerations regarding the geometry of the bearing or external ring lead to a slightly different analysis from that of classical lubrication theory.

2.3. Non-Circular Bearing Model

Considering a ring or a bearing with a deformed surface, a model where its bore is a function of the circumferential coordinate can be proposed. Hence, an expression for the ring bore (R) can be defined as written in Eq. (6).

$$R(\theta) = R_0 + f(\theta) \quad (6)$$

where $f(\theta)$ is an arbitrary function that represents the surface irregularity, and R_0 is the nominal radius.

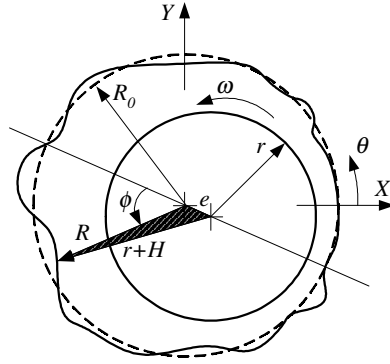


Figure 3. Geometry of a deformed ring

The irregularity function must be smooth to avoid sudden contractions or enlargements. These abrupt changes in the film thickness cause pressure drops or rises due to inertia effects. As stated before, these effects are not included in the model.

The film thickness can be calculated from the hatched triangle on Fig (3), defined by the eccentricity (e), and the sides R and $(r + H)$. The application of the cosine rule of triangles gives:

$$e^2 + R^2 + 2eR \cos \phi = (r + H)^2 \quad (7)$$

Where ϕ is the angle measured from the location of maximum film thickness. Substitution of Eq. (7) in Eq. (6) yields:

$$e^2 + R_0^2 + 2R_0 f + f^2 + 2eR_0 \cos \phi + 2ef \cos \phi = r^2 + 2rH + H^2 \quad (8)$$

Conveniently, the ring nominal radius is defined as the shaft radius added to a nominal radial clearance (c_r), as stated by Eq. (9).

$$R_0 = r + c_r \quad (9)$$

The ratio between the radial clearance and the shaft radius is usually very small. Thus, after substitution of Eq. (9) into Eq. (8), the second-order terms involving c_r and the other variables of the same order (e , H , f) can be discarded, yielding:

$$H = c_r + f + e \cos \phi \quad (10)$$

Equation (10) represents the film thickness as the difference between the ring and the shaft radius ($R-r$), expressed by the first two terms, combined to the location of the shaft center, as already expected. It can also be noticed that the thickness is function of an angle based on a non-stationary coordinate system. For convenience, a change to a referential fixed in the center of the ring is done. From Fig. (2), it is possible to write the following relationship of the angular coordinates, where β is the journal attitude angle with respect to the X axis.

$$\phi = \pi - \beta + \theta \quad (11)$$

Substitution of Eq. (11) in Eq. (10) yields:

$$H = c_r + f - e(\cos \theta \cos \beta + \sin \theta \sin \beta) \quad (12)$$

The eccentricity components relative to the X and Y directions of the fixed coordinate system are:

$$e_x = e \cos \beta \quad (13)$$

$$e_y = e \sin \beta \quad (14)$$

To perform the simulation, it can be considered that the journal motion is synchronous, as if driven by unbalance, and the eccentricity e has a constant value. Then, the attitude angle β is equal to ωt . However, there is no impediment to simulate other types of motion.

Finally, substitution of Eq. (13) and Eq. (14) in Eq. (12) yields the expression that determines the thickness of the fluid layer in relation to the fixed coordinates:

$$H(\theta, t) = c_r + f(\theta) - e_x(t) \cos \theta - e_y(t) \sin \theta \quad (15)$$

To complete the statement of the pressure field expression, the gradients of the film thickness are necessary:

$$\frac{\partial H}{\partial t} = -\dot{e}_x \cos \theta - \dot{e}_y \sin \theta \quad (16)$$

and

$$\frac{\partial H}{\partial \theta} = f' + e_x \sin \theta - e_y \cos \theta \quad (17)$$

where,

$$f' = \frac{df}{d\theta}$$

and

$$\dot{e}_i = \frac{de_i}{dt}, \quad i = X, Y.$$

Substitution of Eq. (15), Eq. (16) and Eq. (17) into Eq. (5) gives the expression that determines the pressure field:

$$p(\theta, z, t) = 3\mu \left[\frac{(\omega e_x - 2\dot{e}_y) \sin \theta - (\omega e_y + 2\dot{e}_x) \cos \theta + \omega f'}{(c_r + f - e_x \cos \theta - e_y \sin \theta)^3} \right] \left(z^2 - \frac{L^2}{4} \right) \quad (18)$$

The pressure field expression is almost the same as the presented by Kirk and Gunter (1976). The only difference is the introduction of the term with the irregularity function. From Eq. (18) some important observations can be made. When the ring is perfectly circular the pressure will be null if the journal is centered within the ring, i.e., $e = 0$. However, for the ring with deformed geometry, even if the eccentricity is null, pressure will be generated.

3. Computational Results

To illustrate the pressure field behavior due to the irregularities some computational results are presented in this section. The simulations performed consider only synchronous motion of the journal when not centered. In all subsequent simulations the pressure will be evaluated at the middle plane of the ring, i.e., $z = 0$. The data used in the simulations are given in Tab. 1.

Table 1. Parameters for the simulations

Journal angular velocity (rpm)	480
Nominal radial clearance (mm)	2
Length of the ring (mm)	200
Viscosity of the lubricant (Ns/m ²)	0,04

In the first simulation presented, an irregularity function that creates only some local deformations is employed, as defined by Eq. (19). The constants A and k_1 are chosen to adjust the form and frequency of irregularities. In this first case $A = 0,1c_r$ and $k_1 = 4$

$$f(\theta) = \begin{cases} A \sin^2(k_1 \theta), & 90^\circ < \theta < 135^\circ \text{ ou } 270^\circ < \theta < 315^\circ \\ -A \sin^2(k_1 \theta), & 180^\circ < \theta < 225^\circ \end{cases} \quad (19)$$

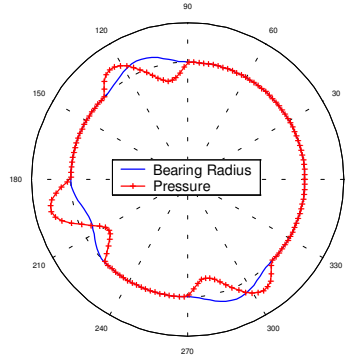


Figure 4. Ring deformation and pressure distribution

Figure 4 depicts the geometry of the external ring and the pressure field generated when there is no motion of the journal's center, i.e., the eccentricity is null. Note that the pressure rises in the convergent areas and drops along the divergent ones.

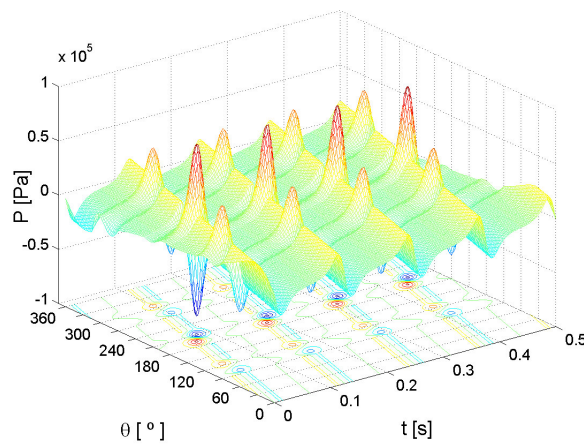


Figure 5. Pressure distribution

Including the journal synchronous motion, the pressure has a different value at each time instant. The graph presented in Fig. 5 is the combination of the pressure of Fig. 4 with the result that is obtained for plain journal bearings.

At the following simulation Eq. (20) is applied to describe irregularities along the whole $[0, 2\pi]$ domain.. The parameters used for this function were: $A = 0,1c_r$, $a = 0,5$, $b = 0,2$, $k_1 = 1$, $k_2 = 9$, $k_3 = 5$.

$$f(\theta) = A(a \cos(k_1\theta) \sin(k_2\theta) + b \cos(k_3\theta)) \quad (20)$$

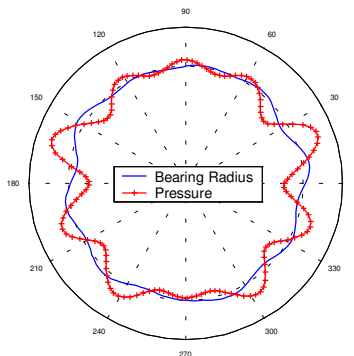


Figure 6. Ring deformation and pressure distribution

The results obtained with this function are qualitatively similar to those of the previous case, as observed in Fig. 6 and Fig. 7. The importance of these results is to show the agreement with the classical lubrication theory, and how the non-circular ring produces significant differences in the pressure distribution.

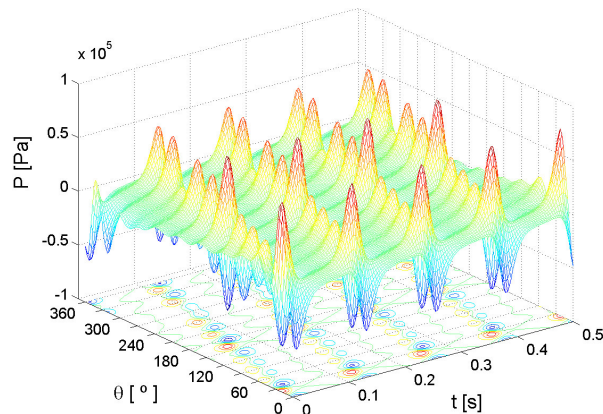


Figure 7. Pressure distribution

The pressure variation at three different locations of the ring for this last case, representing a possible measurement with transducers positioned in its circumference, is presented in Fig. 8. The acquisition of these signals is important to detect the behavior of the dynamic forces caused by the pressure field.

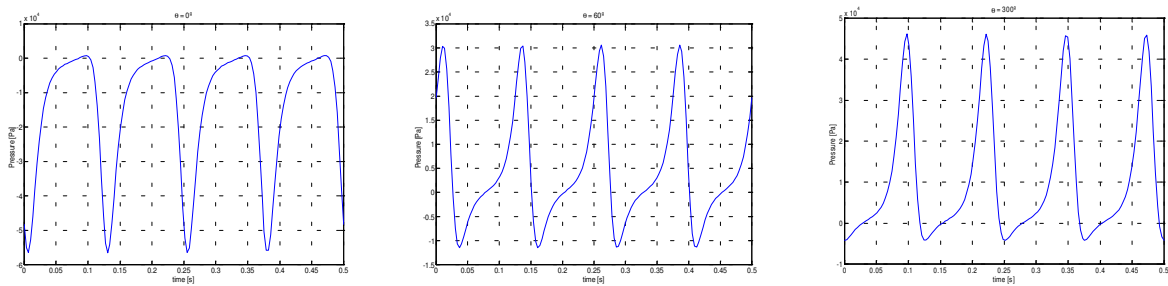


Figure 8. Pressure variation in three locations of the ring

An analysis of these signals in the frequency domain, as shown in Fig. 9, may reveal other harmonics that compose the excitation. As the integration of the pressure distribution yields the force acting on the rotating shaft, these force components may be introduced on a rotordynamic model in order to perform simulations to analyse the machine behavior under these conditions.

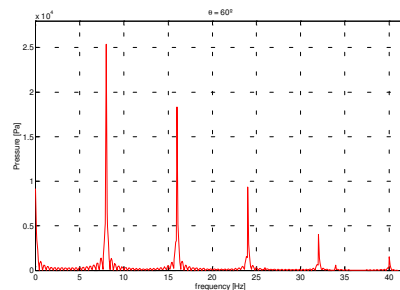


Figure 9. FFT of a pressure signal

4. Turbulent Flow Effects.

As mentioned on section 2, one of the hypotheses made during the statement of the Reynolds equation pointed out the laminar nature of the flow. Depending of the fluid viscosity and of journal rotation speed the flow may be turbulent

and this effect must be taken into account. As shown by Childs (1993), and Allaire et al (1985), it is possible to model the effects of the turbulence with a modified Reynolds equation, according to Eq. (21).

$$\frac{1}{r^2} \frac{\partial}{\partial \theta} \left(\frac{H^3}{\mu} G_\theta \frac{\partial p}{\partial \theta} \right) + \frac{\partial}{\partial z} \left(\frac{H^3}{\mu} G_z \frac{\partial p}{\partial z} \right) = \frac{\omega}{2} \frac{\partial H}{\partial \theta} + \frac{\partial H}{\partial t} \quad (21)$$

where

$$G_\theta = (12 + 0,0136R_e^{0,90})^{-1}, \quad G_z = (12 + 0,0043R_e^{0,96})^{-1}, \quad R_e = r\omega \frac{\rho}{\mu} H$$

This modification is based on eddy viscosity effects, through the addition of the parameters G_θ and G_z that are functions of the local Reynolds number. Hence, the quotients μ/G_θ and μ/G_z may be viewed as effective local viscosities. Note that for small Reynolds numbers (Re), Eq. (21) reassumes the form of Eq. (1).

Applying the same procedure of the Ocvirk solution to Eq. (21) the resultant pressure field is given by:

$$p = \frac{\mu}{4G_z} \left[\frac{(\omega e_x - 2\dot{e}_y) \sin \theta - (\omega e_y + 2\dot{e}_x) \cos \theta + \omega f'}{(c_r + f - e_x \cos \theta - e_y \sin \theta)^3} \right] \left(z^2 - \frac{L^2}{4} \right) \quad (22)$$

Eq. (22) doesn't differ a lot of that obtained with laminar flow formulation. In fact, the turbulent flow correction modifies only the magnitude of the pressure field.

5. Conclusions

The model proposed to identify deviations of the circular geometry in a hydrodynamic component seems to be coherent with the presented theory. The results presented are more qualitative and intend only to associate the pressure generation mechanism to the geometry of the component. The knowledge of how the pressure is distributed along the deformed component allows a comparison to the original one and then the geometry changes can be located.

The identification of the real geometry of the component requires a more sophisticated model, using numerical methods as FEM and CFD. Other effects, as axial flow and inertia effects, must also be taken into account to create a more complete and reliable model. Experimental data should also be taken to validate the model and verify the agreement of the numerical results.

6. References

- Allaire, P. E., Kocur, J. A., Nicholas, J. C., 1985, "A Pressure-Parameter Method for Finite-Element Solutions of Reynolds' Equation", ASLE Trans Vol. 28, No. 2, pp. 150-158.
- Allaire, P. E., Nicholas, J. C., Gunter, E. J., "Systems of Finite Elements for Finite Bearings," ASME Journal of Lubrication Technology, Vol. 98, No. 2, April 1977, pp. 187-197
- Childs, D.W., 1993, "Turbomachinery Rotordynamics—Phenomena, Modeling and Analysis", John Wiley & Sons Inc.
- Kirk, R.G. and Gunter, E. J., 1976, "Short Bearing Analysis Applied to Rotor Dynamics, Part 1: Theory", Journal of Lubrication Technology, Vol 98(1), pp. 47-56.
- San Andres, L., 2000, "Lubrication Theory Class Notes", <http://www.mengr.tamu.edu:70/mechanics-systems/lsanandres/me626/notes/default.htm>.
- Vance, J. M., 1988, "Rotordynamics of Turbomachinery", John Wiley & Sons Inc.

7. Responsibility notice

The authors are the only responsible for the printed material included in this paper.